JACS
JOURNAL OF THE AMERICAN CHEMICAL SOCIETY
Communication
Cite This: J. Am. Chem. Soc. 2019, 141, 12967−12973
pubs.acs.org/JACS

Synthesis and Magnetism of Neutral, Linear Metallocene Complexes of Terbium(II) and Dysprosium(II)

Colin A. Gould,[†,§] K. Randall McClain,[‡,§] Jason M. Yu,[¶] Thomas J. Groshens,[‡] Filipp Furche,*[,¶] Benjamin G. Harvey,*[,‡] and Jeffrey R. Long*[,†,∥,⊥]

[†]Department of Chemistry and [∥]Department of Chemical and Biomolecular Engineering, University of California, Berkeley, Berkeley, California 94720, United States

[‡]U.S. Navy, Naval Air Warfare Center, Weapons Division, Research Department, Chemistry Division, China Lake, California 93555, United States

[¶]Department of Chemistry, University of California, Irvine, 1102 Natural Sciences II, Irvine, California 92697-2025, United States

[⊥]Materials Sciences Division, Lawrence Berkeley National Laboratory, Berkeley, California 94720, United States

Supporting Information

ABSTRACT: The divalent metallocene complexes Ln(Cp^{iPr5})$_2$ (Ln = Tb, Dy) were synthesized through the KC_8 reduction of Ln(Cp^{iPr5})$_2$I intermediates and represent the first examples of neutral, linear metallocenes for these elements. X-ray diffraction analysis, density functional theory calculations, and magnetic susceptibility measurements indicate a $4f^n5d^1$ electron configuration with strong s/d mixing that supports the linear coordination geometry. A comparison of the magnetic relaxation behavior of the two divalent metallocenes relative to salts of their trivalent counterparts, [Ln(Cp^{iPr5})$_2$][B(C$_6$F$_5$)$_4$], reveals that lanthanide reduction has opposing effects for dysprosium and terbium, with magnetic relaxation times increasing from Tb^{III} to Tb^{II} and decreasing from Dy^{III} to Dy^{II}. The impact of this effect is most notably evident for Tb(Cp^{iPr5})$_2$, which displays an effective thermal barrier to magnetic relaxation of 1205 cm^{-1} and a 100-s blocking temperature of 52 K, the highest values yet observed for any nondysprosium single-molecule magnet.

Lanthanide elements possess contracted valence 4f orbitals, a characteristic that impacts both molecular structure and magnetism.[1] These core-like orbitals engage in weak, predominantly electrostatic interactions with ligands and are therefore nearly degenerate in energy, giving rise to unparalleled single-ion magnetic anisotropies in lanthanide complexes.[2,3] Due to the electrostatic nature of the 4f−ligand interactions, steric constraints tend to dictate molecular structure and coordination geometry can be challenging to predict.[4] This situation is in contrast to transition metal complexes, where covalent interactions between ligands and diffuse valence d orbitals typically quench orbital angular momentum, but lead to predictable geometries.[5]

Fine control over coordination geometry is essential to the design of single-molecule magnets. For instance, increasing the axiality of the ligand field can maximize the thermal barrier to magnetization reversal (U_{eff}) for oblate Dy^{III} and Tb^{III} ions and reduce transverse anisotropy, which can, in turn, decrease the rate of through-barrier relaxation.[6,7] Enforcing a high symmetry is also important, particularly for complexes containing lanthanide ions with integer spin (non-Kramers ions)—such as Tb^{III}—for which $\pm M_J$ degeneracy is not guaranteed.[8]

Recent studies have demonstrated that molecular complexes containing Ln^{II} centers can be isolated across the entire lanthanide series and that these ions can in some instances possess $4f^n5d^1$ electron configurations.[9,10] We reasoned that such an electronic structure might enable the synthesis of complexes with predictable, high-symmetry geometries—arising from covalent interactions between ligands and the valence 5d electron—that also maintain the high anisotropy imparted by the $4f^n$ electrons. As complexes of the type [Dy(Cp^R)$_2$]$^+$ possess the highest operating temperatures reported to date for single-molecule magnets, we chose to study the effect of metal reduction on bis(cyclopentadienyl) lanthanide complexes.[11] Increasing the axial symmetry in such molecules could enhance magnetic properties and this approach could also provide a valuable opportunity to study the impact of reducing Ln^{III} to Ln^{II} on single-molecule magnet behavior.

Molecules containing nontraditional Ln^{II} centers are still quite rare and are mostly limited to trigonal, anionic [Ln(L)$_3$]$^-$ complexes with L = C$_5$H$_4$SiMe$_3$, C$_5$H$_3$(SiMe$_3$)$_2$, or N(SiMe$_3$)$_2$.[9] In designing a synthetic route to neutral, divalent lanthanide metallocenes, we identified reports of the reduction of Ln(Cp^{ttt})$_2$I (Ln = Tm, Dy; Cp^{ttt} = 1,2,4-tri(*tert*-butyl)cyclopentadienyl).[12] Reduction of Tm(Cp^{ttt})$_2$I with KC_8 in a nonpolar solvent enabled isolation of the bent THF adduct Tm(Cp^{ttt})$_2$(THF), while reduction of Dy(Cp^{ttt})$_2$I was only successful in the presence of 18-crown-6, leading to an iodide-bridged "ate" complex (Cp^{ttt})$_2$Dy(μ-I) K(18-crown-6).[12] We reasoned that a Ln(Cp^R)$_2$I intermediate containing the more strongly donating, bulkier, and more symmetric pentaisopropylcyclopentadienyl (Cp^{iPr5}) ligand could facilitate clean reduction to Ln(Cp^R)$_2$ species.

In order to make direct comparisons between neutral and cationic complexes, we synthesized the terbium(III) complex

Received: May 30, 2019
Published: August 2, 2019

DOI: 10.1021/jacs.9b05816
J. Am. Chem. Soc. 2019, 141, 12967−12973

Scheme 1. Synthetic Routes to the Terbium(III) Metallocenium Salt 1 and Lanthanide(II) Metallocene Complexes 2 and 3

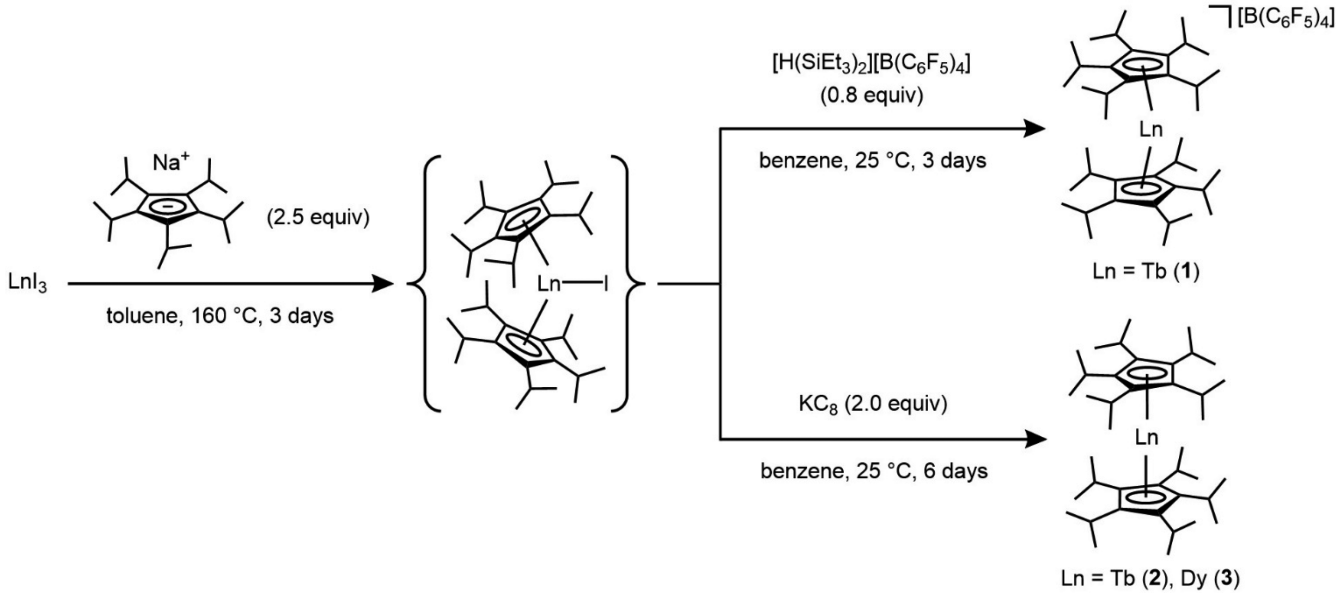

salt $[Tb(Cp^{iPr5})_2][B(C_6F_5)_4]$ (**1**) via iodide abstraction from $Tb(Cp^{iPr5})_2I$, in a procedure analogous to the synthesis of $[Dy(Cp^{iPr5})_2][B(C_6F_5)_4]$ (Scheme 1).[11d] Crucially, reduction of $Ln(Cp^{iPr5})_2I$ (Ln = Tb, Dy) in benzene with KC_8 and subsequent crystallization from hexane afforded orange-amber crystals of $Ln(Cp^{iPr5})_2$ (Ln = Tb (**2**), Dy (**3**)), the first neutral, linear metallocenes for any divalent lanthanide more reducing than samarium(II) (Scheme 1).[13] Both **2** and **3** are indefinitely stable under argon in the solid state and hexane solution at 25 °C, in contrast to the aforementioned $[Ln(L)_3]^-$ complexes, which are prone to decomposition at ambient temperatures.[9b]

The solid-state structures of **1**−**3** were determined by single-crystal X-ray diffraction analyses (Figure 1). Although the cyclopentadienyl rings in **1** are nearly parallel, the Tb^{III} site is situated slighty off-center, with an average Cp−Tb−Cp angle of 159.8(4)°. The metal center is disordered over four positions, analogous to the disorder observed in $[Dy(Cp^{iPr5})_2][B(C_6F_5)_4]$.[11d] In contrast, the metal ions in **2** and **3** are located on an inversion center, resulting in a Cp−Ln−Cp angle of 180° and Cp−Ln−Cp core symmetry (excluding isopropyl groups) of D_{5d}. The high-symmetry structures of **2** and **3** are significant, as most $4f^n$ lanthanide metallocenes are bent.[14−16]

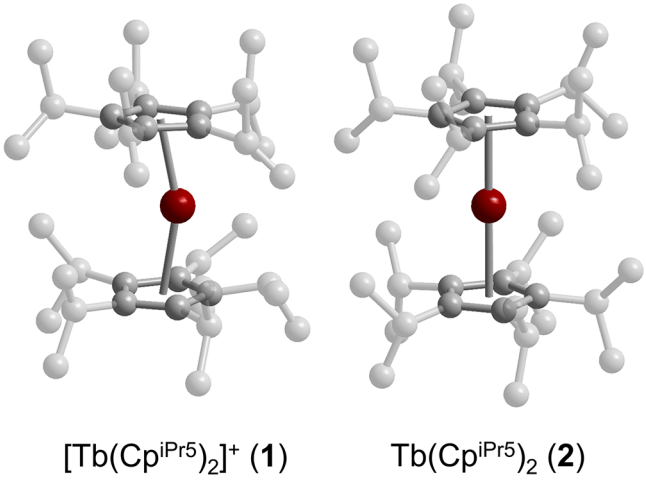

Figure 1. Solid-state molecular structures of **1** and **2**. Maroon and gray spheres represent Tb and C atoms, respectively; hydrogen atoms, the $[B(C_6F_5)_4]^-$ counteranion in **1**, and positional disorder are omitted for clarity. Compound **3** is isostructural to **2**.

The solid-state structures of **1**−**3** can also provide insight into electronic configuration. In $[LnCp^R_3]^-$ complexes featuring Ln^{II} centers with $4f^{n+1}$ configurations, the Ln−Cp^R (centroid) distances are larger than those of the trivalent analogues by 0.1−0.2 Å. In contrast, for Ln^{II} centers with $4f^n5d^1$ configurations, the increase in the Ln−Cp^R distance is much smaller, 0.02−0.05 Å.[9] The average Tb−Cp distance in **1** is 2.356(6) Å, lengthening to 2.416(1) Å in **2**, while the average Dy−Cp distance in $[Dy(Cp^{iPr5})_2][B(C_6F_5)_4]$ is 2.336(4) Å, lengthening to 2.385(1) Å in **3**. A similar trend is observed for the average Ln−C distance. The average Tb−C distances in **1** and **2** are 2.635(8) and 2.704(2) Å, respectively, and the average Dy−C distances in $[Dy(Cp^{iPr5})_2][B(C_6F_5)_4]$ and **3** are 2.621(2) and 2.673(4) Å, respectively. These differences support a $4f^n5d^1$ configuration for **2** and **3**.[9c,f,g,17,18]

Density functional theory (DFT) calculations performed on optimized structures of $Tb(Cp^{iPr5})_2$ and $Dy(Cp^{iPr5})_2$ afforded ^8A (in C_1 symmetry) and $^7A_1$ (in D_5 symmetry) ground terms, respectively, corresponding to a $4f^n5d^1$ configuration (see Supporting Information for details). These calculations support a nondegenerate highest occupied molecular orbital (HOMO) with significant $5d_{z2}$ character (Figure 2). Natural population analysis revealed that the HOMO also has considerable 6s character due to $5d_{z2}$-6s orbital mixing.[19] Covalent σ-bonding interactions between these metal-based orbitals and the cyclopentadienyl ligands likely support the linear coordination geometry observed for these divalent metallocenes. The lowest unoccupied molecular orbital (LUMO) is doubly degenerate and has significant d_{xy}/d_{x2-y2} character, consistent with the orbital ordering found in ferrocene.[20]

The dc magnetic susceptibility data were collected for **1**−**3** from 2 to 300 K under an applied magnetic field of 1000 Oe (Figures S13−S18). The room temperature $\chi_M T$ value for **1** is 11.96 emu K/mol, which agrees well with the expected value of

DOI: 10.1021/jacs.9b05816
J. Am. Chem. Soc. 2019, 141, 12967−12973

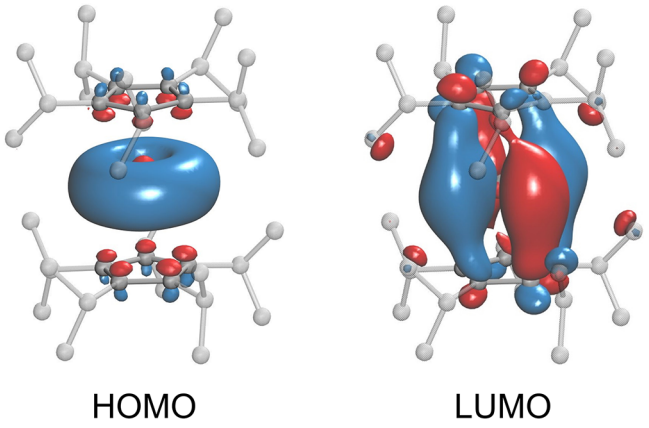

Figure 2. HOMO (left, 170Aα, contour value 0.03) and LUMO (right, 172Aα, contour value 0.03) for **2** with hydrogen atoms excluded for clarity. The HOMO and LUMO for **3** are isolobal.

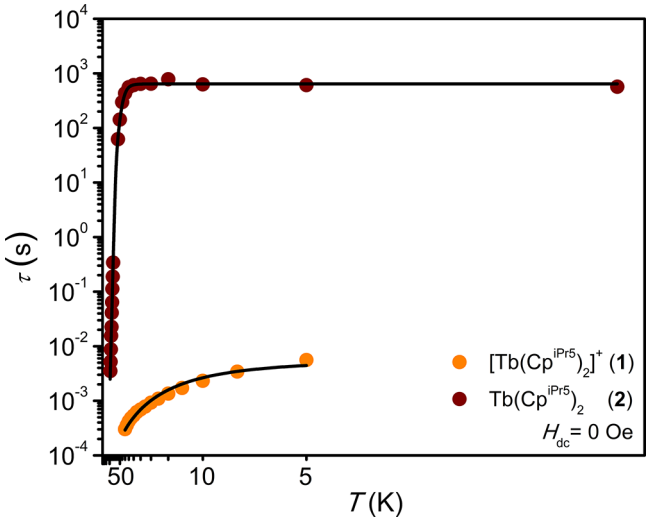

Figure 3. Plot of magnetic relaxation time (τ, log scale) versus temperature (T, inverse scale) for polycrystalline samples of **1** (yellow) and **2** (maroon). Black lines represent fits to the data.

11.82 emu K/mol for a free Tb^{III} ion ($4f^8$). Slightly larger values were found for the divalent complexes: 12.72 emu K/mol for **2** and 15.15 emu K/mol for **3**. These values are distinct from the values of 14.13 and 14.07 emu K/mol predicted for a $4f^9$ Tb^{II} ion and a $4f^{10}$ Dy^{II} ion, respectively. Previously reported Ln^{II} complexes with $4f^n5d^1$ configurations follow an $L-S$ coupling scheme, resulting in room temperature $\chi_M T$ values close to the predicted values of 14.42 and 17.01 emu K/mol for Tb^{II} and Dy^{II}, respectively.[9f−h] The values for **2** and **3** are substantially lower, suggesting a deviation from $L-S$ coupling that can be explained by the strong $5d_{z^2}-6s$ mixing. Indeed, gas-phase spectra of Ln^{2+} ions with $4f^n6s^1$ configurations reveals that these ions follow a $j-j$ coupling scheme due to weak spin−spin coupling between the 4f and 6s orbitals.[21,22] Evaluating the nature of such complex electronic structures is challenging and we are currently pursuing further insights through a variety of spectroscopic measurements.

Magnetic relaxation in **1**−**3** was probed by ac magnetic susceptibility and dc magnetic relaxation experiments (Figures S19−S58). Under zero dc field, a polycrystalline sample of compound **1** exhibited peaks in the out-of-phase susceptibility (χ_M'') between 2 and 40 K, indicative of slow magnetic relaxation. Pronounced curvature in a corresponding plot of magnetic relaxation time (τ, log scale) versus T (inverse scale) is indicative of Raman relaxation (Figure 3, yellow symbols).[23] Magnetic relaxation is ∼5 orders of magnitude faster in **1** than in $[Dy(Cp^{iPr5})_2][B(C_6F_5)_4]$, consistent with previous reports on $[Ln(Cp^{ttt})_2][B(C_6F_5)_4]$ (Ln = Tb, Dy).[11d,24] This result can be attributed to the noninteger spin of Tb^{III}, which enables mixing of the ground $\pm M_J$ pseudodoublet that can promote rapid through-barrier relaxation.[24]

A polycrystalline sample of compound **2** exhibited frequency-dependent χ_M'' signals under zero dc field from 74 to 92 K. The data could be fit to an Orbach mechanism with a large effective barrier to magnetic relaxation of U_{eff} = 1205 cm^{-1} (Figure S61). Additionally, a 100-s magnetic blocking temperature (T_b) of 52 K was extracted from dc relaxation experiments (Figure 3, maroon symbols). The values of U_{eff} and T_b for **2** are the highest yet reported for any single-molecule magnet that is not a dysprosium(III) complex and are only surpassed by the complex $[Dy(O^tBu)_2(py)_5][BPh_4]$ and molecules of the type $[Dy(Cp^R)_2]^+$.[8f,11,25,26] The substantial increase of over 5 orders of magnitude in the magnetic relaxation times of **2** as compared to **1** can be attributed to at least two factors. Reduction from terbium(III), a non-Kramers ion, to terbium(II), a Kramers ion, enforces degeneracy of the ground $\pm M_J$ doublet in **2**.[27] In addition, increasing the axial symmetry of the coordination environment should reduce transverse anisotropy, suppressing tunneling of the magnetization.

Lanthanide reduction has the opposite effect on magnetic relaxation in the dysprosium metallocene complexes. A polycrystalline sample of **3** does not display slow magnetic relaxation on the time scale of dc magnetic relaxation experiments (τ > 50 s), although a 100-s magnetic blocking temperature of 5 K could be extracted from data obtained for a dilute (28 mM) toluene solution of **3**. This blocking temperature is substantially lower than the value of T_b = 56 K observed for $[Dy(Cp^{iPr5})_2][B(C_6F_5)_4]$, likely due to conversion from dysprosium(III), a Kramers ion, to dysprosium(II), a non-Kramers ion.[11d] While fast compared to $[Dy(Cp^{iPr5})_2][B(C_6F_5)_4]$, the rate of magnetic relaxation in **3** is nearly 10^4 times slower than observed for **1**, underscoring the importance of axial symmetry in complexes containing non-Kramers ions.[8a]

Magnetic hysteresis measurements further confirmed the trends in magnetic relaxation behavior observed for **1**−**3**. While hysteresis is largely absent for **1**, even at 2 K (Figure S71), **2** exhibits open magnetic hysteresis loops at zero field up to 55 K (Figure 4). Surprisingly, the coercive field for **2** increases from 2 to 30 K (Figure S73), implying that the rate of magnetic relaxation decreases with increasing temperature. Indeed, dc relaxation measurements performed on polycrystalline **2** and a dilute (19 mM) toluene solution of **2** revealed that the relaxation time increases slightly from 2 to 15 K (Tables S3 and S5).[28] Polycrystalline **3** exhibits butterfly magnetic hysteresis from 2 to 75 K (Figures S78−S80), while measurements performed on a dilute (28 mM) toluene solution of **3** revealed hysteresis loops that are open at zero field as high as 10 K (Figures S81 and S82). Significantly, compounds $Tb(Cp^{iPr5})_2$ and $Dy(Cp^{iPr5})_2$ represent the first single-molecule magnets based on a divalent lanthanide ion to show magnetic hysteresis.[29] Importantly, unlike $[Dy(Cp^R)_2]^+$ salts, these charge-neutral molecules may also be stable to

DOI: 10.1021/jacs.9b05816
J. Am. Chem. Soc. 2019, 141, 12967−12973

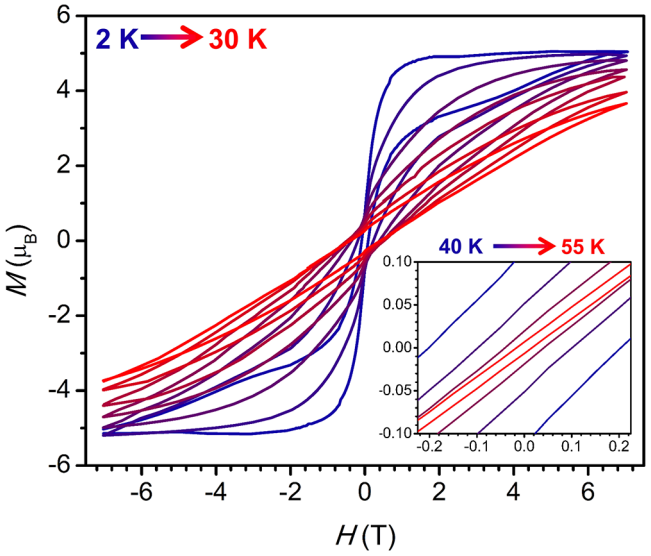

Figure 4. Magnetic hysteresis data for **2** collected at a sweep rate of 14.7(1) mT/s for $H > 2$ T and 3.9(2) mT/s for $H < 2$ T.

sublimation, offering a ready means of depositing them onto surfaces and within devices.

In order to investigate the unusual low-temperature hysteresis behavior, magnetic relaxation in **2** and **3** was probed by ac susceptibility measurements from 2 to 20 K. The resulting data reveal complicated relaxation dynamics featuring multiple relaxation processes (Figures S60–S70), which persist in data collected on dilute solution samples of each compound. This behavior likely arises from the complex electronic structure of the divalent metallocenes, and clearly warrants further investigation.[30]

The foregoing results demonstrate that lanthanide reduction in bis(pentaisopropyl)cyclopentadienyl metallocenes has a substantial impact on both the coordination geometry and magnetic properties. In particular, the $4f^n5d^1$ electronic configuration of $Ln(Cp^{iPr5})_2$ supports axial, high-symmetry structures, likely a result of enhanced covalency in metal–ligand interactions. Notably, the more axial symmetry of $Dy(Cp^{iPr5})_2$ results in higher hysteresis temperatures relative to $[Tb(Cp^{iPr5})_2]^+$, although both complexes feature non-Kramers ions. Reduction of terbium(III) to terbium(II) also results in a drastic enhancement of the magnetic relaxation time for $Tb(Cp^{iPr5})_2$ and gives rise to the highest thermal barrier to magnetic inversion and highest magnetic blocking temperature yet observed for a nondysprosium single-molecule magnet. In total, these results highlight the utility of lanthanide redox chemistry in modulating magnetic relaxation. We are currently pursuing a more detailed understanding of the complex electronic structure and magnetism of these new divalent metallocenes via a variety of spectroscopic methods.

■ ASSOCIATED CONTENT

Supporting Information

The Supporting Information is available free of charge on the ACS Publications website at DOI: 10.1021/jacs.9b05816.

Synthesis of **1**–**3**, IR spectroscopy, UV–vis spectroscopy, crystallographic data, magnetic characterization, and DFT calculations (PDF)

Data for $C_{40}H_{70}Tb$, $BC_{24}F_{20}$ (CIF)

Data for $C_{40}H_{70}Dy$ (CIF)

Data for $C_{40}H_{70}Tb$ (CIF)

■ AUTHOR INFORMATION

Corresponding Authors

*jrlong@berkeley.edu

*benjamin.g.harvey@navy.mil

*filipp.furche@uci.edu

ORCID

Colin A. Gould: 0000-0001-9539-1582

K. Randall McClain: 0000-0001-8072-8402

Filipp Furche: 0000-0001-8520-3971

Benjamin G. Harvey: 0000-0003-2091-3539

Jeffrey R. Long: 0000-0002-5324-1321

Author Contributions

§K.R.M. and C.A.G. contributed equally to this work.

Notes

The authors declare no competing financial interest.

■ ACKNOWLEDGMENTS

This work was supported by NSF grant CHE-1800252 (J.R.L., C.A.G.), the Naval Air Warfare Center, Weapons Division (NAWCWD) PL-219 program (B.G.H., K.R.M., T.J.G.), and NSF grant CHE-1800431 (F.F., J.M.Y.). We thank the National Science Foundation Graduate Research Fellowship Program for support of C.A.G. and J.M.Y. and we thank Dr. Katie R. Meihaus for editorial assistance.

■ REFERENCES

(1) (a) Meyer, G. *The Rare Earth Elements: Fundamentals and Applications*; Atwood, D. A., Ed.; Wiley: Chichester, U. K., 2012. (b) Cotton, S. A. *Lanthanide and Actinide Chemistry*; Wiley: Chichester, U. K., 2006.

(2) (a) Dieke, G. H. *Spectra and Energy Levels of Rare Earth Ions in Crystals*; Crosswhite, H. M., Crosswhite, H., Eds.; Wiley: New York, 1968. (b) Freeman, A. J.; Watson, R. E. Theoretical Investigation of Some Magnetic and Spectroscopic Properties of Rare-Earth Ions. *Phys. Rev.* **1962**, *127*, 2058–2075. (c) Gatteschi, D.; Sessoli, R.; Villain, J. *Molecular Nanomagnets*; Oxford University Press: Oxford, 2006.

(3) (a) Lucas, J.; Lucas, P.; Le Mercier, T.; Rollat, A.; Davenport, W. G. *Rare Earths: Science, Technology, Production and Use*; Elsevier, 2014. (b) Ishikawa, N.; Sugita, M.; Ishikawa, T.; Koshihara, S.-Y.; Kaizu, Y. Lanthanide Double-Decker Complexes Functioning as Magnets at the Single-Molecular Level. *J. Am. Chem. Soc.* **2003**, *125*, 8694–8695.

(4) (a) Cotton, S. A.; Harrowfield, J. M. *Lanthanides: Coordination Chemistry in Encyclopedia of Inorganic and Bioinorganic Chemistry*; Wiley: New York, 2011. (b) Moeller, T. Coordination Chemistry of the Lanthanide Elements- One Hundred Years of Development and Understanding. *Adv. Chem. Ser.* **1967**, *62*, 306–317. (c) Bombieri, G. New Trends in the Structural Chemistry of Actinide and Lanthanide Coordination Compounds. *Inorg. Chim. Acta* **1987**, *139*, 21–32.

(5) (a) Emeleus, H. J.; Sharpe, A. G. *Modern Aspects of Inorganic Chemistry*, 4th ed.; Wiley: New York, 1973. (b) Marks, T. J.; Ernst, R. D. *Comprehensive Organometallic Chemistry*; Wilkinson, G., Stone, F. G. A., Abel, E. W., Eds.; Pergamon: Oxford, U. K., 1982.

(6) (a) Rinehart, J. D.; Long, J. R. Exploiting Single-Ion Anisotropy in the Design of f-Element Single-Molecule Magnets. *Chem. Sci.* **2011**, *2*, 2078–2085. (b) Chilton, N. F.; Collison, D.; McInnes, E. J. L.; Winpenny, R. E. P.; Soncini, A. An electrostatic model for the determination of magnetic anisotropy in dysprosium complexes. *Nat. Commun.* **2013**, *4*, 2551. (c) Sievers, J. Z. Asphericity of 4*f*-shells in their Hund's rule ground states. *Z. Phys. B: Condens. Matter Quanta* **1982**, *45*, 289–296. (d) Ungur, L.; Chibotaru, L. F. Magnetic anisotropy in the excited states of low symmetry lanthanide

DOI: 10.1021/jacs.9b05816
J. Am. Chem. Soc. 2019, 141, 12967–12973

complexes. *Phys. Chem. Chem. Phys.* **2011**, *13*, 20086. (e) Chilton, N. F.; Goodwin, C. A. P.; Mills, D. P.; Winpenny, R. E. P. The first near-linear bis(amide) f-block complex: a blueprint for a high temperature single molecule magnet. *Chem. Commun.* **2015**, *51*, 101.

(7) (a) Day, B. M.; Guo, F.-S.; Layfield, R. A. Cyclopentadienyl Ligands in Lanthanide Single-Molecule Magnets: One Ring to Rule Them All? *Acc. Chem. Res.* **2018**, *51*, 1880−1889. (b) Habib, F.; Brunet, G.; Vieru, V.; Korobkov, I.; Chibotaru, L. F.; Murugesu, M. Significant Enhancement of Energy Barriers in Dinuclear Dysprosium Single-Molecule Magnets Through Electron-Withdrawing Effects. *J. Am. Chem. Soc.* **2013**, *135*, 13242−13245.

(8) (a) Liu, J.-L.; Chen, Y.-C.; Tong, M.-L. Symmetry Strategies for high performance lanthanide-based single-molecule magnets. *Chem. Soc. Rev.* **2018**, *47*, 2431−2453. (b) Chen, Y.-C.; Liu, J.-L.; Ungur, L.; Liu, J.; Li, Q.-W.; Wang, L.-F.; Ni, Z.-P.; Chibotaru, L. F.; Chen, X.-M.; Tong, M.-L. Symmetry-Supported Magnetic Blocking at 20 K in Pentagonal BipyramidalDy(III) Single-Ion Magnets. *J. Am. Chem. Soc.* **2016**, *138*, 2829−2837. (c) Gupta, S. K.; Rajeshkumar, T.; Rajaraman, G.; Murugavel, R. An air-stable Dy(III) single-ion magnet with high anisotropy barrier and blocking temperature. *Chem. Sci.* **2016**, *7*, 5181−5191. (d) Gregson, M.; Chilton, N. F.; Ariciu, A.-M.; Tuna, F.; Crowe, I. F.; Lewis, W.; Blake, A. J.; Collison, D.; McInnes, E. J. L.; Winpenny, R. E. P.; Liddle, S. T. A monometallic lanthanide bis(methanediide) single molecule magnet with a large energy barrier and complex spin relaxation behavior. *Chem. Sci.* **2016**, *7*, 155−165. (e) Liu, J.; Chen, Y.-C.; Liu, J.-L.; Vieru, V.; Ungur, L.; Jia, J.-H.; Chibotaru, L. F.; Lan, Y.; Wernsdorfer, W.; Gao, S.; Chen, X.-M.; Tong, M.-L. A Stable Pentagonal BipyramidalDy(III) Single-Ion Magnet with a Record Magnetization Reversal Barrier over 1000 K. *J. Am. Chem. Soc.* **2016**, *138*, 5441−5450. (f) Ding, Y.-S.; Chilton, N. F.; Winpenny, R. E. P.; Zheng, Y.-Z. On Approaching the Limit of Molecular Magnetic Anisotropy: A Near-Perfect Pentagonal BipyramidalDysprosium(III) Single-Molecule Magnet. *Angew. Chem., Int. Ed.* **2016**, *55*, 16071−16074. (g) Meihaus, K. R.; Long, J. R. Magnetic Blocking at 10 K and a Dipolar-Mediated Avalanche in Salts of the Bis(η^8-cyclooctatetraenide) Complex $[Er(COT)_2]^-$. *J. Am. Chem. Soc.* **2013**, *135*, 17952−17957. (h) Ungur, L.; Le Roy, J. J.; Korobkov, I.; Murugesu, M.; Chibotaru, L. F. Fine-tuning the Local Symmetry to Attain Record Blocking Temperature and Magnetic Remanence in a Single-Ion Magnet. *Angew. Chem., Int. Ed.* **2014**, *53*, 4413−4417. (i) Sørensen, M. A.; Hansen, U. B.; Perfetti, M.; Pedersen, K. S.; Bartolomé, E.; Simeoni, G. G.; Mutka, H.; Rols, S.; Jeong, M.; Zivkovic, I.; Retuerto, M.; Arauzo, A.; Bartolomé, J.; Piligkos, S.; Weihe, H.; Doerrer, L. H.; van Slageren, J.; Rønnow, H. M.; Lefmann, K.; Bendix, J. Chemical tunnel-splitting-engineering in a dysprosium-based molecular nanomagnet. *Nat. Commun.* **2018**, *9*, 1292−1301.

(9) (a) MacDonald, M. R.; Bates, J. E.; Fieser, M. E.; Ziller, J. W.; Furche, F.; Evans, W. J. Expanding Rare-Earth Oxidation State Chemistry to Molecular Complexes of Holmium(II) and Erbium(II). *J. Am. Chem. Soc.* **2012**, *134*, 8420−8423. (b) MacDonald, M. R.; Bates, J. E.; Ziller, J. W.; Furche, F.; Evans, W. J. Completing the Series of + 2 Ions for the Lanthanide Elements: Synthesis of Molecular Complexes of Pr^{2+}, Gd^{2+}, Tb^{2+}, and Lu^{2+}. *J. Am. Chem. Soc.* **2013**, *135*, 9857−9868. (c) Fieser, M. E.; MacDonald, M. R.; Krull, B. T.; Bates, J. E.; Ziller, J. W.; Furche, F.; Evans, W. J. Structural, Spectroscopic, and Theoretical Comparison of Traditional vs Recently Discovered Ln^{2+} Ions in the $[K(2.2.2\text{-cryptand})][(C_5H_4SiMe_3)_3Ln]$ Complexes: The Variable Nature of Dy^{2+} and Nd^{2+}. *J. Am. Chem. Soc.* **2015**, *137*, 369−382. (d) Evans, W. J. Tutorial on the Role of Cyclopentadienyl Ligands in the Discovery of Molecular Complexes of the Rare-Earth and Actinide Metals in New Oxidation States. *Organometallics* **2016**, *35*, 3088−3100. (e) Fieser, M. E.; Palumbo, C. T.; La Pierre, H. S.; Halter, D. P.; Voora, V. K.; Ziller, J. W.; Furche, F.; Meyer, K.; Evans, W. J. Comparisons of lanthanide/actinide + 2 ions in a tris(aryloxide)arene coordination environment. *Chem. Sci.* **2017**, *8*, 7424−7433. (f) Huh, D. H.; Darago, L. E.; Ziller, J. W.; Evans, W. J. Utility of Lithium in Rare-Earth Metal Reduction Reactions to Form Nontraditional Ln^{2+} Complexes and Unusual $[Li(2.2.2\text{-cyrptand})]^{1+}$ Cations. *Inorg. Chem.* **2018**, *57*, 2096−2102. (g) Ryan, A. J.; Darago, L. E.; Balasubramani, S. G.; Chen, G. P.; Ziller, J. W.; Furche, F.; Long, J. R.; Evans, W. J. Synthesis, Structure, and Magnetism of Tris(amide) $[Ln\{N(SiMe_3)_2\}_3]^{1-}$ Complexes of the Non-traditional + 2 Lanthanide Ions. *Chem. - Eur. J.* **2018**, *24*, 7702−7709. (h) Meihaus, K. R.; Fieser, M. E.; Corbey, J. R.; Evans, W. J.; Long, J. R. Record High Single-Ion Magnetic Moments through $4f^n5d^1$ Electron Configurations in the Divalent Lanthanide Complexes $[(C_5H_4SiMe_3)_3Ln]^-$. *J. Am. Chem. Soc.* **2015**, *137*, 9855−9860.

(10) Evans, W. J. The Importance of Questioning Scientific Assumptions: Some Lessons from f Element Chemistry. *Inorg. Chem.* **2007**, *46*, 3435−3449.

(11) (a) Goodwin, C. A. P.; Ortu, F.; Reta, D.; Chilton, N. F.; Mills, D. P. Molecular magnetic hysteresis at 60 K in dysprosocenium. *Nature* **2017**, *548*, 439−442. (b) Guo, F.-S.; Day, B. M.; Chen, Y.-C.; Tong, M.-L.; Mansikkamäki, A.; Layfield, R. A. A Dysprosium Metallocene Single-Molecule Magnet Functioning at the Axial Limit. *Angew. Chem., Int. Ed.* **2017**, *56*, 11445−11449. (c) Guo, F.-S.; Day, B. M.; Chen, Y.-C.; Tong, M.-L.; Mansikkamäki, A.; Layfield, R. A. Magnetic hysteresis up to 80 K in a dysprosium metallocene single-molecule magnet. *Science* **2018**, *362*, 1400−1403. (d) McClain, K. R.; Gould, C. A.; Chakarawet, K.; Teat, S. J.; Groshens, T. J.; Long, J. R.; Harvey, B. G. High-temperature magnetic blocking and magneto-structural correlations in a series of dysprosium(III) metallocenium single-molecule magnets. *Chem. Sci.* **2018**, *9*, 8492−8503.

(12) (a) Jaroschik, F.; Nief, F.; Ricard, L. Synthesis of a new stable, neutral organothulium(II) complex by reduction of a thulium(III) precursor. *Chem. Commun.* **2006**, *4*, 426−428. (b) Jaroschik, F.; Nief, F.; Le Goff, X.-F.; Ricard, L. Isolation of Stable Organodysprosium-(II) Complexes by Chemical Reduction of Dysprosium(III) Precursors. *Organometallics* **2007**, *26*, 1123−1125.

(13) Sitzmann, H.; Dezember, T.; Schmitt, O.; Weber, F.; Wolmershäuser, G.; Ruck, M. Metallocenes of Samarium, Europium, and Ytterbium with the Especially Bulky Cyclopentadienyl Ligands $C_5H(CHMe_2)_4$, $C_5H_2(CMe_3)_3$, and $C_5(CHMe_2)_5$. *Z. Anorg. Allg. Chem.* **2000**, *626*, 2241−2244.

(14) (a) Evans, W. J.; Hughes, L. A.; Hanusa, T. P. Synthesis and crystallographic characterization of an unsolvated, monomeric samarium bis(pentamethylcyclopentadienyl) organolanthanide complex, $(C_5Me_5)_2Sm$. *J. Am. Chem. Soc.* **1984**, *106*, 4270−4272. (b) Visseaux, M.; Barbier-Baudry, D.; Blacque, O.; Hafid, A.; Richard, P.; Weber, F. New base-free metallocenes of samarium and neodymium, an approach to stereoelectronic control in organo-lanthanide chemistry. *New J. Chem.* **2000**, *24*, 939−942. (c) Weber, F.; Sitzmann, H.; Schultz, M.; Sofield, C. D.; Andersen, R. A. Synthesis and Solid State Structures of Sterically Crowded d^0-Metallocenes of Magnesium, Calcium, Strontium, Barium, Samarium, and Ytterbium. *Organometallics* **2002**, *21*, 3139−3146. (d) Evans, W. J.; Perotti, J. M.; Brady, J. C.; Ziller, J. W. Tethered Olefin Studies of Alkene versus Tetraphenylborate Coordination and Lanthanide Olefin Interactions in Metallocenes. *J. Am. Chem. Soc.* **2003**, *125*, 5204−5212. (e) Nocton, G.; Ricard, L. N-aromatic heterocycle adducts of bulky $[1,2,4\text{-}(Me_3C)_3C_5H_2]_2Sm$: synthesis, structure and solution analysis. *Dalton Trans* **2014**, *43*, 4380−4387. (f) Kilpatrick, A. F. R.; Cloke, F. G. N. A base-free synthetic route to anti-bimetallic lanthanide pentalene complexes. *Dalton Trans* **2017**, *46*, 5587−5597. (g) Palumbo, C. T.; Ziller, J. W.; Evans, W. J. Structural characterization of the bent metallocenes, $[C_5H_3(SiMe_3)_2]_2Sm$ and $[C_5H_3(CMe_3)_2]_2Ln$ (Ln = Eu, Sm), and the mono(cyclopentadienyl) tetraphenylborate complex, $[C_5H_3(CMe_3)_2]Eu(\mu\text{-}\eta^6\text{:}\ \eta^1\text{-}Ph)_2BPh_2$. *J. Organomet. Chem.* **2018**, *867*, 142−148. (h) Ruspic, C.; Moss, J. R.; Schürmann, M.; Harder, S. Remarkable Stability of Metallocenes with Superbulky Ligands: Spontaneous Reduction of Sm^{III} to Sm^{II}. *Angew. Chem., Int. Ed.* **2008**, *47*, 2121−2126. (i) van Velzen, N. J. C.; Harder, S. Deca-Arylsamarocene: An Unusually Inert Sm(II) Sandwich Complex. *Organometallics* **2018**, *37*, 2263−2271. (j) Kaupp, M.; Schleyer, P. v. R.; Dolg, M.; Stoll, H. The Equilibrium Structures of Monomeric Group 2 and Lanthanide(II) Metallocenes MCp_2 (M =

DOI: 10.1021/jacs.9b05816
J. Am. Chem. Soc. 2019, 141, 12967−12973

Ca, Sr, Ba, Sm, Eu, Yb) Studied by ab Initio Calculations. *J. Am. Chem. Soc.* **1992**, *114*, 8202−8208.
(15) For instance, values of the Cp−Sm−Cp angle in $Sm(Cp^R)_2$ complexes range from 132.7 to 180°, depending on the steric profile of the ligand (ref 14). Even in $Sm(Cp^{BIG})_2$ (Cp^{BIG} = $C_5(4\text{-}n\text{Bu-}C_6H_4)_5^-$), which has a Cp−Sm−Cp angle of 180°, displacement parameters for the Sm^{II} center in the structure are expanded in the plane between the cyclopentadienyl ligands, suggesting that metal coordination may deviate from linearity (refs 14h, i). Displacement parameters for the Ln^{II} centers in **2** and **3** are not expanded in this manner, however, suggesting that the metal ions remain localized in a high-symmetry position.
(16) Complexes **2** and **3** form as a mixture of *rac* and *meso* isomers, defined by different orientations of the methyl carbons of the isopropyl groups. The position of the metal atom, the carbon atoms in the cyclopentadienyl rings, and the methine carbon atoms in the isopropyl groups are identical for the two isomers in the crystal structure of **2** and **3**.
(17) Evans, W. J.; Allen, N. T.; Ziller, J. W. The Availability of Dysprosium Diiodide as a Powerful Reducing Agent in Organic Synthesis: Reactivity Studies and Structural Analysis of $DyI_2(DME)_3$ and Its Naphthalene Reduction Product. *J. Am. Chem. Soc.* **2000**, *122*, 11749−11750.
(18) The $4f^95d^1$ electron configuration for **3** expands the known coordination geometries in which dysprosium(II) adopts a $4f^95d^1$ configuration instead of the classical $4f^{10}$ configuration (refs 9c, 17).
(19) Reed, A. E.; Weinstock, R. B.; Weinhold, F. Natural Population Analysis. *J. Chem. Phys.* **1985**, *83*, 735−746.
(20) Ishimura, K.; Hada, M.; Nakatsuji, H. Ionized and excited states of ferrocene: Symmetry adapted cluster-configuration-interaction study. *J. Chem. Phys.* **2002**, *117*, 6533.
(21) (a) Wybourne, B. G. *Spectroscopic Properties of the Rare Earths*; Interscience: New York, 1965. (b) Bryant, B. W. Spectra of Doubly and Triply Ionized Ytterbium, Yb III and Yb IV. *J. Opt. Soc. Am.* **1965**, *55*, 771−779.
(22) The magnetic moments of divalent lanthanide complexes with $4f^n5d^1$ configurations (refs 9f−h) have previously been rationalized according to a formalism introduced by Cloke and co-workers: Anderson, D. M.; Cloke, F. G. N.; Cox, P. A.; Edelstein, N.; Green, J. C.; Pang, T.; Sameh, A. A.; Shalimoff, G. On the Stability and Bonding in Bis(η-arene)lanthanide Complexes. *J. Chem. Soc., Chem. Commun.* **1989**, 53−55 One potential scenario considered according to this formalism is a "coupled configuration" in which spin−spin coupling between 4f and 5d electrons dominates and the combined spin from the 5d and 4f orbitals, $S = 1/2 + S_{4f}$, couples with the 4f orbital angular momentum, L, to give rise to a total angular momentum, J. This is analogous to a traditional L−S coupling scheme. A second potential scenario considered in this formalism is an "uncoupled configuration" in which spin−spin coupling between the 4f and 5d electrons is weak. In this scenario, the spin of the 4f electrons, S_{4f}, couples with the 4f electron orbital angular momentum, L, to generate a total angular momentum J, which then couples to the $S = 1/2$ contributed by the 5d electron ($L = 0$), leading to predicted room temperature $\chi_M T$ values of 12.20 and 14.51 emu K/mol for Tb^{II} ($4f^85d^1$; $L = 3$, $S = 3$ for $4f^8$; $L = 0$, $S = 1/2$ for $5d^1$) and Dy^{II} ($4f^95d^1$; $L = 5$, $S = 5/2$ for $4f^9$; $L = 0$, $S = 1/2$ for $5d^1$) ions, respectively. These predicted values more closely match those obtained for **2** and **3**. The term "uncoupled configuration" is somewhat misleading in this case, as the 4f and 5d spins are still coupled, albeit weakly. The electronic structure is perhaps better described by a j−j coupling scheme in which the L−S coupling in individual shells is stronger than the spin-spin interactions between shells (the same requirement laid out by Cloke and co-workers for the "uncoupled configuration"). Such j−j coupling has been observed in the gas-phase spectroscopy of divalent lanthanide ions with $4f^n5d^1$ and $4f^n6s^1$ configurations (see ref 21). .
(23) (a) Liddle, S. T.; van Slageren, J. Improving f-element single molecule magnets. *Chem. Soc. Rev.* **2015**, *44*, 6655−6669. (b) Woodruff, D. N.; Winpenny, R. E. P.; Layfield, R. A. Lanthanide Single-Molecule Magnets. *Chem. Rev.* **2013**, *113*, 5110−5148.
(24) Goodwin, C. A. P.; Reta, D.; Ortu, F.; Liu, J.; Chilton, N. F.; Mills, D. P. Terbocenium: completing a heavy lanthanide metallocenium cation family with an alternative anion abstraction strategy. *Chem. Commun.* **2018**, *54*, 9182−9185.
(25) (a) Liu, F.; Velkos, G.; Krylov, D. S.; Spree, L.; Zalibera, M.; Ray, R.; Samoylova, N. A.; Chen, C.-H.; Rosenkranz, M.; Schiemenz, S.; Ziegs, F.; Nenkov, K.; Kostanyan, A.; Greber, T.; Wolter, A. U. B.; Richter, M.; Büchner, B.; Avdoshenko, S. M.; Popov, A. A. Air-stable redox-active nanomagnets with lanthanide spins radical- bridged by a metal-metal bond. *Nat. Commun.* **2019**, *10*, 571−582. (b) Velkos, G.; Krylov, D. S.; Kirkpatrick, K.; Spree, L.; Dubrovin, V.; Büchner, B.; Avdoshenko, S. M.; Bezmelnitsyn, V.; Davis, S.; Faust, P.; Duchamp, J.; Dorn, H. C.; Popov, A. A. High Blocking Temperature of Magnetization and Giant Coercivity in the Azafullerene $Tb_2@C_{79}N$ with a Single-Electron Terbium−Terbium Bond. *Angew. Chem., Int. Ed.* **2019**, *58*, 5891−5896.
(26) For reference, the current record values are U_{eff} = 1541 cm^{-1} and T_b = 65 K, as observed for $[Dy(Cp^{iPr5})(Cp^*)][B(C_6F_5)_4]$ (Cp^* = pentamethylcyclopentadienyl) (ref 11c).
(27) Kramers' theorem states that a time-reversal symmetric system with half-integer total spin will have eigenstates that are at least doubly degenerate. For lanthanide ions with half-integer values of S, this means that the ground $\pm M_J$ doublet will be degenerate and resistant to direct mixing between the two projections, mitigating through-barrier magnetic relaxation processes. The ground states obtained by DFT calculations for **2** and **3** are ^8A and $^7A_1$(or ^7A_g), respectively, and on this basis we assign **2** as a Kramers ion ($S = 7/2$, noninteger spin) and **3** as a non-Kramers ion ($S = 3$, integer spin). Kramers, H. A. *Proc. Amsterdam Acad.* **1930**, *33*, 959.
(28) A decrease in the rate of magnetic relaxation with increasing temperature was also observed for $U(H_2BPz_2)_3$, although the magnetic relaxation process in this case was found to arise from intermolecular dipolar interactions, rather than the behavior of individual molecules. The relaxation process in **2** that decreases in rate with increasing temperature appears to be molecular in origin, as it is replicated in measurements on a dilute (19 mM) toluene solution of **2** with an average Tb···Tb separation of 44 Å. (a) Rinehart, J. D.; Meihaus, K. R.; Long, J. R. Observation of a Secondary Slow Relaxation Process for the Field-Induced Single-Molecule MagnetU-$(H_2BPz_2)_3$. *J. Am. Chem. Soc.* **2010**, *132*, 7572−7573. (b) Meihaus, K. R.; Rinehart, J. D.; Long, J. R. Dilution-Induced Slow Magnetic Relaxation and Anomalous Hysteresis in Trigonal Prismatic Dysprosium(III) and Uranium(III) Complexes. *Inorg. Chem.* **2011**, *50*, 8484−8489.
(29) Xémard, M.; Cordier, M.; Molton, F.; Duboc, C.; Le Guennic, B.; Maury, O.; Cador, O.; Nocton, G. Divalent Thulium Crown Ether Complexes with Field-Induced Slow Magnetic Relaxation. *Inorg. Chem.* **2019**, *58*, 2872−2880.
(30) Multiple relaxation processes are often ascribed to the presence of two or more distinct metal sites in a molecule (refs 30a−c). While **1**−**3** are synthesized as a mixture of *rac* and *mer* isomers, it seems unlikely that subtle changes in the orientation of remote methyl groups would cause such large changes in the rate of magnetic relaxation. Multiple relaxation processes have also been observed for a mononuclear single-molecule magnet featuring a single metal environment (ref 30d). DFT calculations conducted on **2** and **3** reveal an excited state (^6A for **2** and ^5A_g or $^5A_1$ for **3**) ∼4 kcal/mol higher in energy than the ground state. The $\pm M_J$ manifold of this excited state may be close enough to mix with the $\pm M_J$ manifold of the ground state, leading to a complex electronic structure that could perhaps complicate the relaxation dynamics of the divalent metallocenes. (a) Blagg, R. J.; Ungur, L.; Tuna, F.; Speak, J.; Comar, P.; Collison, D.; Wernsdorfer, W.; McInnes, E. J. L.; Chibotaru, L. F.; Winpenny, R. E. P. Magnetic relaxation pathways in lanthanide single-molecule magnets. *Nat. Chem.* **2013**, *5*, 673−678. (b) Liu, C. M.; Xiong, J.; Zhang, D.-Q.; Wang, B.-W.; Zhu, D.-B. Multiple thermal magnetic relaxation in a two-dimensional ferromagnetic dysprosium-(III) metal-organic framework. *RSC Adv.* **2015**, *5*, 104854−104861. (c) Wang, W.-M.; Kang, X.-M.; Shen, H.-Y.; Wu, Z.-L.; Gao, H.-L.;

DOI: 10.1021/jacs.9b05816
J. Am. Chem. Soc. 2019, 141, 12967−12973

Cui, J.-Z. Modulating single-molecule magnet behavior towards multiple relaxation processes through structural variation in Dy_4 clusters. *Inorg. Chem. Front.* **2018**, *5*, 1876−1885. (d) Jeletic, M.; Lin, P.-H.; Le Roy, J. J.; Korobkov, I.; Gorelsky, S. I.; Murugesu, M. An Organometallic Sandwich Lanthanide Single-Ion Magnet with an Unusual Multiple Relaxation Mechanism. *J. Am. Chem. Soc.* **2011**, *133*, 19286−19289.

DOI: 10.1021/jacs.9b05816
J. Am. Chem. Soc. 2019, 141, 12967−12973